EPR study of Ni^+ centers in SrF_2

P. J. Alonso
Departamento de Física Fundamental, Universidad de Zaragoza, Zaragoza, Spain and Consejo Superior de Investigaciones Cientificas, Facultad Ciencias, Universidad de Zaragoza, Zaragoza, Spain
J. Casas González
Departamento de Optica, Facultad Ciencias, Universidad de Zaragoza, Zaragoza, Spain
H. W. den Hartog
Solid State Physics Laboratory, 1, Melkweg, Groningen, The Netherlands
R. Alcalá
Departamento de Optica, Facultad Ciencias, Universidad de Zaragoza, Zaragoza, Spain
(Received 22 July 1982)

The EPR spectra of two kinds of Ni^+ centers created by room-temperature x irradiation of SrF_2:Ni single crystals are reported. One of them labeled as Ni^+-I shows a pure tetragonal symmetry with a g tensor given by the values $g_{||}=2.597\pm0.005$ and $g_{\perp}=2.092\pm0.005$. The superhyperfine (SHF) structure is interpreted as due to the interaction with four equivalent fluorines. The interaction with each of these fluorines is given by an axial tensor with $A_{||}=235\pm5$ MHz and $A_{\perp}=105\pm5$ MHz. The other type of Ni^+ centers labeled as Ni^+-II shows a slight orthorhombic distortion with respect to the tetragonal symmetry. The principal values of their g tensor are $g_x=2.093\pm0.005$, $g_y=2.087\pm0.005$, and $g_z=2.589\pm0.005$ and the orientation of the principal axes is given by the Euler angles $\phi=45°$, $\theta=2°$, and $\Psi=0°$ with respect to the cube axes. The observed SHF structure is interpreted in the same way as for Ni^+-I centers but with $A_{||}=250\pm5$ MHz and $A_{\perp}=100\pm5$ MHz. The basic model for both defects is a Ni^+ ion displaced along one of the $\langle 100\rangle$ directions from the center of the cube of fluorines toward one of its faces, forming a kind of NiF_4^{3-} molecular ion. The slight orthorhombic distortion of Ni^+-II centers is likely to be due to the presence of an extra defect in the neighborhood of Ni^+ ions. The production and stability of both kinds of defects under different treatments is also reported. From these results and by comparison with optical absorption data we have concluded that Ni^+-I centers are responsible for an absorption band at 270 nm and that Ni^+-II centers produce an absorption band at 285 nm.

I. INTRODUCTION

From the beginning of the last decade considerable effort has been devoted to the study of the spectroscopic properties of 3*d* ions in fluorite-type crystals (CaF_2, SrF_2, BaF_2, CdF_2, and $SrCl_2$). A review paper about the results obtained in these kinds of studies has been recently published.[1]

Some changes in these spectroscopic properties can be produced by exposing the crystals to ionizing radiations. These changes are due either to the formation of complex centers consisting of a lattice defect close to an impurity ion or to modifications in the valence state of the impurity. Similar effects were observed a few years ago in fluorite-type crystals doped with rare-earth-metal impurities.[2–6]

In the last few years we have been performing a systematic study of impurity-related centers created by x irradiation of 3*d* ion-doped fluorite-type crystals. In all of the studied systems we have found that substitutional divalent 3*d* ions are reduced by x irradiation to the monovalent state, so, the reduction of Co^{2+} to Co^+ and the x-ray-induced transformation of Mn^{2+} to Mn^+ have been observed in CaF_2 and SrF_2.[7–10]

In a recent paper[11] we have presented the optical properties of x-irradiated CaF_2:Ni and SrF_2:Ni. In that work it was reported that an absorption band of complex structure peaking at about 275 nm appears after room-temperature (RT) x irradiation of SrF_2:Ni, and it was proposed that the center responsible for this band should be a Ni^+ ion. From the complex structure of this absorption band and from its bleaching behavior it was concluded that at least

 ©1983 The American Physical Society

two different kinds of Ni^+ centers were present. By comparison with the results in CaF_2:Ni and taking into account that in this material Ni^+ centers have been characterized by EPR techniques,[12] it was suggested that the basic configuration of this defect in SrF_2 should be a Ni^+ ion situated in an off-center position displaced along one of the ⟨100⟩ directions of the crystal.

In order to check this model we have undertaken an EPR study of RT x-irradiated SrF_2:Ni, and we have found that x irradiation produces different kinds of Ni^+ centers. One of them with tetragonal symmetry has the basic configuration described above. This center will be labeled as Ni^+-I. The other main center has basically the same structure, but its symmetry is lower showing a slightly orthorhombic distortion. It will be labeled as Ni^+-II. We have also performed a comparison of the EPR data with the optical-absorption results, and we have associated an absorption band peaking at 270 nm with the tetragonal Ni^+ centers and another one with its maximum at 285 nm with the orthorhombic defects.

II. EXPERIMENTAL PROCEDURE

Single crystals of SrF_2:Ni were prepared by means of the Bridgman technique using a 25-kW high-frequency generator. The crucible material chosen was high-purity carbon. Ni impurities were added to the starting material as NiF_2. The Ni concentration in the raw material was about 0.4 at. % but, as it has been said elsewhere,[11] the final concentration is believed to be smaller than that.

All the irradiations were performed using a normal-focus Cu-target x-ray tube working at 40 kV and 20 mA. Optical bleachings have been done using a 100-W high-pressure Hg lamp or a 250-W high-pressure Xe lamp. To obtain polarized light a Glan-Thompson quartz prism was used. The optical-absorption measurements were taken with a Cary 17 spectrophotometer.

EPR spectra were measured at 77 K using an immersion quartz Dewar in an E-112 Varian spectrometer working in the x band. The field-modulation frequency was 100 kHz. In order to obtain accurate values of the microwave frequency and the magnetic field, the diphenylpicrylhydrazyl ($g=2.0037$) and the Cr^{3+} and MgO ($g=1.9799$) lines were used as standards, and the correction of the magnetic field was assumed to be linear in all the range.

III. EXPERIMENTAL RESULTS

A. Production and bleaching characteristics

Before irradiation Ni^+ EPR signals were not detected either at RT or at liquid-nitrogen temperature (LNT). After RT x irradiation the EPR spectrum of a SrF_2:Ni sample shows new signals, which will be identified as due to different types of Ni^+ centers. We show in Fig. 1 a typical spectrum of a RT x-irradiated SrF_2:Ni sample, measured at LNT with the magnetic field oriented along a ⟨100⟩ direction.

It can be seen that this EPR spectrum shows two sets of lines. One of these sets is centered at about $g=2.1$ (high-field spectrum) and consists of five lines. Actually they are not single lines, as can be seen in the one at the highest field. We will show later that in this region of the EPR spectrum, the signals corresponding to at least two kinds of slightly different Ni^+ centers are strongly overlapping. The other set of lines is placed at about $g=2.6$ (low-field spectrum) and shows a complex structure. It is composed of at least three groups of five lines. The lines of the two more prominent groups in this region of the spectrum have been labeled as Ni^+-I and Ni^+-II (see Fig. 1) because, as will be discussed in the following sections, these signals correspond to two different kinds of Ni^+ centers. The third group of five lines in this low-field spectrum, which has been labeled as *U*, has always been found to be very small with respect to the other two. In spite of this, it is believed, by comparison with the Ni^+-I and Ni^+-II signals, that the *U* lines are due to a third type of Ni^+ center. We cannot prove this be-

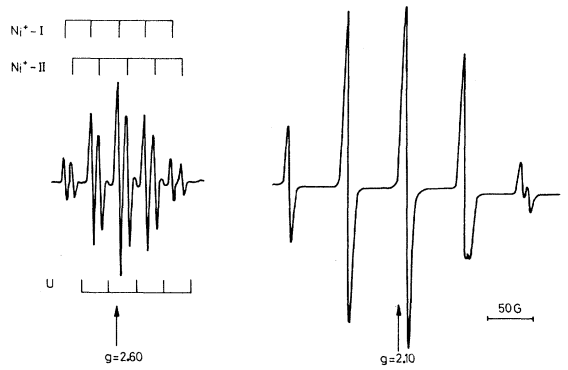

FIG. 1. Typical EPR spectrum of Ni^+ centers observed in a RT x-irradiated SrF_2:Ni sample. Measurement temperature was 80 K. Different lines are grouped in several sets corresponding to different kinds of Ni^+ centers (see text).

cause the *U* signal is too weak, and we have not been able to find any treatment to prepare samples containing predominantly this type of center.

The intensities of the Ni^+-I and Ni^+-II EPR signals, normalized to their saturation values, are given in Fig. 2 as a function of the irradiation time. It is noticeable that the saturation of the Ni^+-I signal takes place at lower dose than the saturation of the Ni^+-II one. In fact, after a short enough x irradiation the Ni^+-I signal is strongly dominant in the EPR spectrum. The saturation of the Ni^+-II signal is not shown in Fig. 2, and it takes place for 10 times longer irradiations.

The behavior of Ni^+-I and Ni^+-II centers is different under optical bleaching. In Fig. 3 the intensities of both signals, normalized to their initial values, are plotted as a function of the bleaching time. The bleaching was performed at RT with the white light from a Xe lamp. We observed that the bleaching is more efficient for Ni^+-I than for Ni^+-II centers. When optical bleaching is performed at LNT we observed a total destruction of the Ni^+-I signal and a limited increase of the Ni^+-II one.

A complementary effect is observed by thermal annealing at 400 K. We show in Fig. 4 the low-field part of the EPR spectrum measured at LNT with the magnetic field along a ⟨100⟩ direction before and after thermal annealing at 400 K for 15 min. It is noticeable that this treatment transforms almost all the type-II Ni^+ centers to type-I centers.

B. EPR of type-I Ni^+ centers

From the preceding section it is clear that after an appropriate treatment we can get a sample with a dominant type-I Ni^+ signal in its EPR spectrum. Under these conditions we have undertaken a study of the evolution of the EPR lines with the orientation of the magnetic field. The observed positions of the Ni^+-I EPR lines for different orientations of of the magnetic field in the (001) plane are given by circles in Fig. 5. In the spectrum taken with the magnetic field parallel to the [100] direction, both the low- and the high-field patterns consist of five lines with relative intensities following approximately the sequence 1:4:6:4:1. If the magnetic field is along the [110] direction, the EPR spectrum consists of two sets of nine lines each, with relative in-

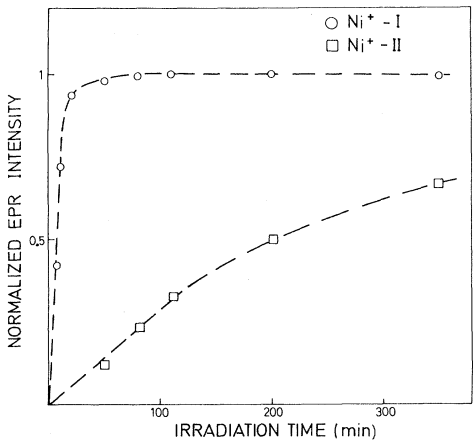

FIG. 2. Intensities, normalized to their saturation value, of Ni^+-I and Ni^+-II EPR signals as a function of irradiation time.

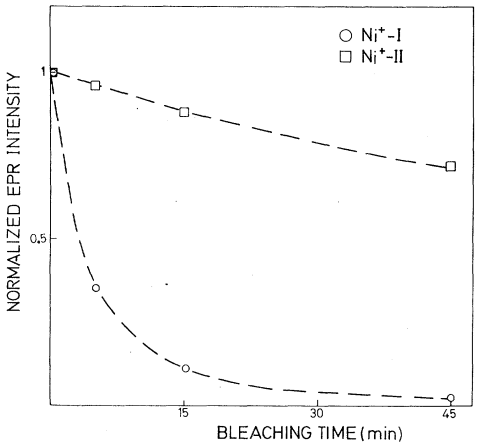

FIG. 3. Intensities, normalized to their initial values, of the Ni^+-I and Ni^+-II EPR signals as a function of bleaching time performed with white light at RT.

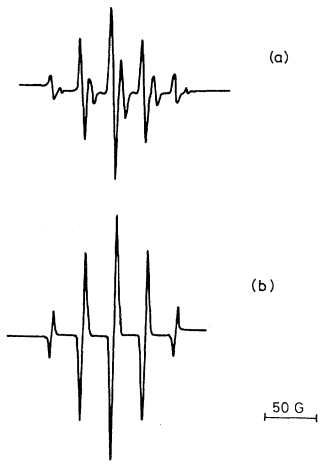

FIG. 4. Low-field EPR spectrum, taken at LNT with the magnetic field along a ⟨100⟩ direction in a RT x-irradiated SrF_2:Ni sample (a) before and (b) after a subsequent annealing at 400 K for 15 min.

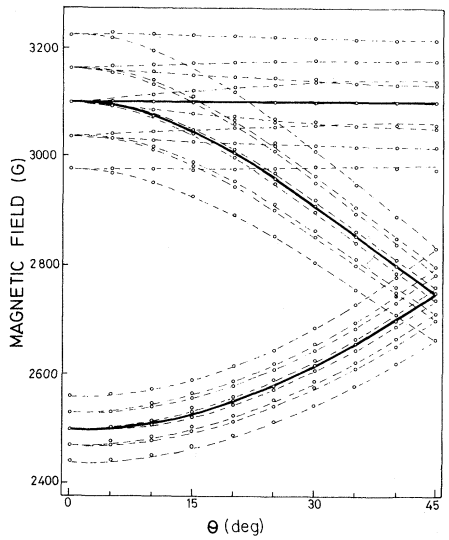

FIG. 5. Circles represent the positions of the observed Ni^+-I EPR lines as a function of the orientation of the magnetic field in the (001) plane. Microwave frequency was 9.08 GHz. Calculated evolution of the EPR lines using the spin Hamiltonian given by (1) with the parameters shown in Table I is represented by broken curves. Central line of each group has been emphasized showing the tetragonal symmetry of the center. Angle θ is measured from the [100] direction.

tensities following approximately the sequence 1:2:2:1:4:1:2:2:1. When the magnetic field is along an arbitrary direction, the EPR spectrum consists of three groups of nine lines each.

The behavior of the central line of each of the three groups as a function of rotation of the crystal can be explained if the center responsible for this EPR spectrum has tetragonal symmetry with its C_4 axis along the $\langle 100 \rangle$ crystal directions. The evolution of these central lines has been marked in Fig. 5.

The observed hyperfine structure suggests that it is due to the interaction with four nuclei with a nuclear spin $I=\frac{1}{2}$, which are equivalent for an orientation of the magnetic field along a $\langle 100 \rangle$ direction. We assume that the nuclei responsible for the hyperfine structure are fluorines because their 100% natural abundance isotope has a nuclear spin $I=\frac{1}{2}$.

In order to analyze the hyperfine structure, several hypotheses have been made: (i) The interaction with each of the four fluorines is described independently (independent bonding model[13]). (ii) The hyperfine interaction with each fluorine has axial symmetry along the bonding direction, Ni^+-F^- line,[14] and consequently this hyperfine interaction can be described by the principal values $A_{||}$ and $A_\perp$ of the hyperfine tensor and the angle α between the bonding direction and the plane of the fluorine ions.

With these hypotheses the following spin Hamiltonian has been used in order to describe the observed EPR spectra:

$$\mathcal{H}=\mu_B[g_{||}H_zS_z+g_\perp(S_xH_x+S_yH_y)] + \sum_{j=1}^{4}[A_\perp(S_{x_j'}I_{x_j'}^{(j)}+S_{y_j'}I_{y_j'}^{(j)})+A_{||}S_{z_j'}I_{z_j'}^{(j)}] \quad (1)$$

with $S=\frac{1}{2}$ and $I^{(j)}=\frac{1}{2}$, and where the (xyz) coordinate system has been chosen with the z direction along the tetragonal axis of the center. The $(x_j'y_j'z_j')$ coordinate system is chosen relative to the j ligand with the z_j' axis along the Ni^+-F^- bonding direction.

Using this spin Hamiltonian we can obtain the best values of its parameters by fitting the calculated positions of the lines to the observed ones. The values obtained in this way are given in Table I. The predicted EPR line positions are shown by dashed lines in Fig. 5.

C. EPR of type-II Ni^+ centers

As we have already said, after RT x irradiation and subsequent optical bleaching at LNT we can get a sample whose Ni^+ EPR spectrum is mainly due to type-II centers. In a sample prepared in such a way, we have measured the evolution of the EPR spectrum with the orientation of the magnetic field. We show in Fig. 6 the rotational diagram corresponding with rotation of the magnetic field in the (001) plane. When the magnetic field is along the [100] direction the EPR spectrum is very similar to the one corresponding with the Ni^+-I centers and consists of two sets of five lines with relative intensities following approximately the sequence 1:4:6:4:1. When the magnetic field is rotated the spectrum becomes more complicated. It can be seen

TABLE I. Spin-Hamiltonian parameters for the Ni^+-I and Ni^+-II centers in SrF_2. The hyperfine constants are given in MHz.

	Ni^+-I	Ni^+-II
g_x	2.092±0.005	2.093±0.005
g_y		2.087±0.005
g_z	2.597±0.005	2.589±0.005
ϵ		2°
$A_{||}$	235 ±5	250 ±5
$A_\perp$	105 ±5	100 ±5
α	10°	10°

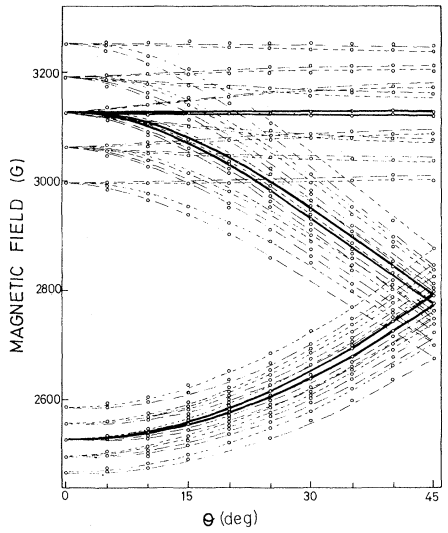

FIG. 6. Circles represent the positions of the observed Ni^+-II EPR lines as a function of the orientation of the magnetic field in the (001) plane. Microwave frequency was 9.14 GHz. Calculated evolution of the EPR lines using the spin Hamiltonian given by (2) with the parameters shown in Table I is represented by the broken curves. Central line of each group has been emphasized (see text). Angle θ is measured from the [100] direction.

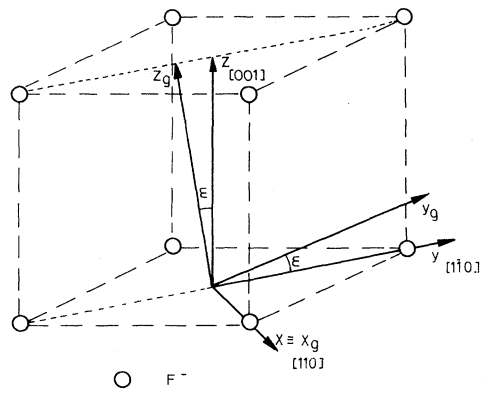

FIG. 7. Orientation of the principal axis (x_g,y_g,z_g) of the g tensor corresponding to the Ni^+-II center. Chosen crystal coordinate system (x,y,z) is also shown. For the sake of clarity a cube of the fluorine sublattice is also displayed.

that each group of lines is composed of two sets of nine lines strongly overlapped. For the sake of clarity we have marked the evolution of the central line of each set. According to this pattern it follows that the point symmetry of the Ni^+-II centers is lower than tetragonal, although the deviation from this symmetry is small. From the analysis of the evolution of these central lines we can get the orientation of the principal axes of the g tensor. They are shown in Fig. 7. One of these principal axes is along the [110] direction (x_g axis) and the other two are in the (110) plane, such that the y_g axis makes an angle ϵ with the [1$\bar{1}$0] direction and the z_g axis makes the angle ϵ with the [001] direction. The rotational diagram shown in Fig. 6 does not provide an unambiguous assignment of the g_x and g_y values, but it can be obtained by analyzing the splitting of the central lines during rotation of the magnetic field in a (110) plane in the neighborhood of the [110] direction.

The analysis of the hyperfine structure has been performed assuming that it is due to the interaction with four fluorine nuclei and using the same hypotheses as in the Ni^+-I case. Consequently, we assume that the hyperfine interactions with the four fluorine nuclei are equivalent in spite of the orthorhombic symmetry of the center. This hypothesis is supported by the observed hyperfine structure: five lines with relative intensities following the sequence 1:4:6:4:1 when the magnetic field is along a ⟨100⟩ direction and nine lines when the magnetic field is along an arbitrary direction in the (001) plane.

With these assumptions we have used the following spin Hamiltonian to describe the experimental results:

$$\mathcal{H}=\mu_B(g_xS_{x_g}H_{x_g}+g_yS_{y_g}H_{y_g}+g_zS_{z_g}H_{z_g}) + \sum_{j=1}^{4}[A_\perp(S_{x_j'}I_{x_j'}^{(j)}+S_{y_j'}I_{y_j'}^{(j)})+A_{||}S_{z_j'}I_{z_j'}^{(j)}] \quad (2)$$

with $S=\frac{1}{2}$ and $I^{(j)}=\frac{1}{2}$, and where the $(x_gy_gz_g)$ coordinate system corresponds to the principal directions of the g tensor (see Fig. 7). The $(x_j'y_j'z_j')$ axes are defined in the same way as for the spin Hamiltonian given by Eq. (1).

By fitting the spin Hamiltonian (2) to our experimental results, we have obtained the best set of values for the parameters that is given in Table I. In Fig. 6 we have represented by dashed lines the calculated line positions using the spin Hamiltonian given by Eq. (2) with the parameters given in Table I.

D. Comparison with the optical-absorption measurements

In a recent paper[11] we have reported the changes in the optical-absorption spectrum of x-irradiated SrF_2:Ni, and we have found that RT x irradiation

induces the formation of a complex absorption band peaked at about 275 nm. The shape of this band indicates that it is composed of at least two strongly overlapped bands in the (270—285)-nm region which were attributed to different kinds of Ni^+ centers. A sample with this complex absorption spectrum (Fig. 8) shows an EPR spectrum as that given in Fig. 1.

As we have already said, a SrF_2:Ni sample whose EPR spectrum shows mainly one of the signals, corresponding either to Ni^+-I or to Ni^+-II centers, can be obtained by appropriate treatments. We show in Fig. 8 the absorption spectrum, in the uv region, corresponding to a crystal in each of these two situtations. When the crystal shows an EPR spectrum due mainly to Ni^+-I centers, the absorption band has its maximum at 270 nm, while in a crystal treated in such a way that its EPR spectrum consists predominantly of Ni^+-II signals the absorption band is centered at about 285 nm.

Recently, we have reported[11] that the absorption spectrum of a RT x-irradiated SrF_2:Ni sample becomes dichroic by optical bleaching at LNT with polarized light in the 275-nm band. Two reorientation stages at about 80 and 170 K have been observed. We have now measured the EPR spectrum of samples containing dominantly either Ni^+-I or Ni^+-II centers before and after LNT optical bleaching in the corresponding absorption band with polarized light having its electric field parallel to the [001] direction, and we have observed an induced dichroism in the EPR spectrum. The thermal reorientations also have been observed following the EPR signals. The reorientation takes place for both kinds of centers at about 170 K. We have not observed any dichroic EPR signal whose reorientation occurs in the 80-K temperature region.

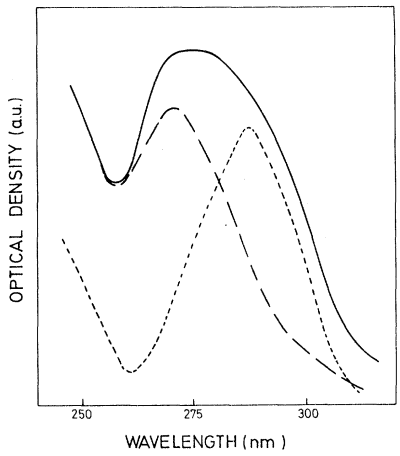

FIG. 8. Optical-absorption spectra of a RT x-irradiated SrF_2:Ni sample (——) without any additional treatment, (— — —) after thermal annealing at 400 K, and (---) after optical bleaching at LNT. Measurements have been performed at LNT.

IV. DISCUSSION

From the correlation we have found between optical and EPR measurements it can be concluded that the absorption band at 270 nm and the tetragonal EPR spectrum are due to one type of center and also that the orthorhombic EPR signal and the 285-nm absorption band are due to another one. As these optical-absorption and EPR signals only appear in Ni-doped SrF_2 after RT x irradiation and not in SrF_2, either pure or doped with other $3d$ ions, we conclude that they are associated with defects related with Ni.

We have proposed elsewhere[11] that the complex absorption band in the 275-nm region is due to the presence of several kinds of Ni^+ centers created by RT x irradiation. We shall show now that this assignation is reinforced by the present results. A basic model for the centers responsible for the EPR and optical-absorption spectrum mentioned above also will be given.

The EPR signals due to both kinds of Ni^+ centers have tetragonal symmetry, except for the slight orthorhombic contribution shown by type-II centers. As we have said, the hyperfine structure is due to the interaction of an electronic spin $S=\frac{1}{2}$ with four equivalent nuclei having a nuclear spin $I=\frac{1}{2}$. Using the same arguments as those employed in the case of tetragonal Ni^+ centers in CaF_2 (Ref. 12) we propose the following basic model: A Ni^+ ion displaced along one of the $\langle 100 \rangle$ directions from the center of the cube of the fluorine ions toward one of its faces forming a kind of NiF_4^{3-} molecular ion (see Fig. 9). The value obtained for the angle α (see Table I) indicates that the NiF_4^{3-} molecule has a pyramidal structure very close to the square planar one. Similar off-center ions in fluorite-structure crystals have also been reported by Moreno[15] in $SrCl_2$:Ag^{2+} and by Bill[16] in $SrCl_2$:Cu^{2+}. It is noticeable that Cu^{2+} is isoelectronic with Ni^+ ($3d^9$) and the outermost electronic configuration of the Ag^{2+} ions is $4d^9$.

The above-described model is a center with C_{4v} point symmetry and is actually the model for a Ni^+-I defect. The structure of the orthorhombic center Ni^+-II is basically the same, but from the pattern of Fig. 6 we conclude that its point symmetry is C_s. From our present results we cannot give a

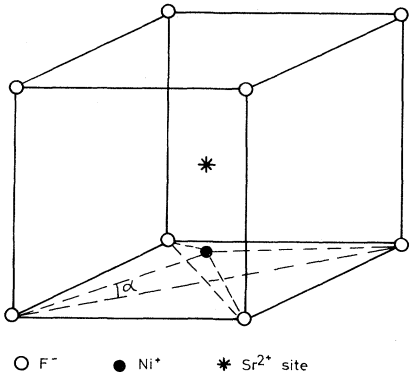

FIG. 9. Basic model for the Ni^+ centers in SrF_2.

conclusive answer to the question concerning the reason for the lower symmetry of the Ni^+-II centers; it could, however, be due to the presence of an extra defect in the vicinity of the Ni^+ ion. The lack of any observable hyperfine interaction with this perturbation prevents us from elucidating its nature.

We will comment now on the spectroscopic properties of our centers. Let us begin with type-I Ni^+ centers. The scheme of energy levels associated with the ground configuration of a complex with C_{4v} symmetry containing a $3d^9$ central ion such as the one given in Fig. 9 is reproduced in Fig. 10.[17] We have chosen the z direction along the tetragonal axis of the defect, and the x and y directions along the diagonal of the ligand square. We want to point out that the x and y axes have been rotated 45° with respect to those given in Ref. 12. The deviations of the g values from the free-electron one are due to the mixing of the ground state with higher excited states. A calculation up to second-order perturbation[17] yields the following expressions for the g values:

$$g_{||}=2-\frac{8\lambda}{\Delta_{||}}-3\left[\frac{\lambda}{\Delta_\perp}\right]^2-\frac{4\lambda^2}{\Delta_{||}\Delta_\perp},$$
$$g_\perp=2-\frac{2\lambda}{\Delta_\perp}-4\left[\frac{\lambda}{\Delta_{||}}\right]^2, \tag{3}$$

where λ is the spin-orbit coupling parameter and the meaning of the energy differences $\Delta_{||}$ and $\Delta_\perp$ is given in Fig. 10. Using these expressions we can get information about the relative positions of the energy levels. From the numbers given in Table I and taking a value of $\lambda=-450\ cm^{-1}$ (Refs. 12 and 17), we obtain the values of $\Delta_{||}=5770\ cm^{-1}$ and $\Delta_\perp=7900\ cm^{-1}$.

The observed Ni^+-I absorption band at 270 nm (approximately 37 000 cm^{-1}) clearly does not correspond with these energy differences. We have not observed any absorption band corresponding with the $\Delta_{||}$ and $\Delta_\perp$ energy differences. This can be due to the fact that the associated transitions are intraconfigurational and probably strongly forbidden. The 270-nm absorption band should correspond with an interconfigurational transition. These kinds of transitions can have a large oscillator strength, and consequently the associated absorption bands are very intense. Interconfigurational transitions have been observed for several $3d$ ions in different matrices.[8–10]

The σ or π character of the electric dipole transition associated with the 270-nm absorption band can be obtained from the changes induced in the EPR signal by optical bleaching with 270-nm polarized light. Since we observe a decrease in the intensity of the signal corresponding to Ni^+-I defects with the tetragonal axis parallel to the direction of the electric field of the bleaching light, we conclude that the 270-nm absorption band corresponds to a transition having a predominantly σ character.

In the case of the Ni^+-II centers we will assume that the orthorhombic distortion only produces a small splitting of the (d_{xz},d_{yz}) level, which is twofold degenerated in the C_{4v} symmetry (see Fig.10). We will neglect the mixing induced in the d functions. With these hypotheses we can make a calculation of the g values as a function of the energy differences Δ_x, Δ_y, and Δ_z given in Fig. 10 and the spin-orbit coupling parameter λ. In order to take into account the second-order corrections, and since g_x and g_y values are very close, we have assumed that the second-order correction is the same as the one corresponding to the tetragonal case taking for

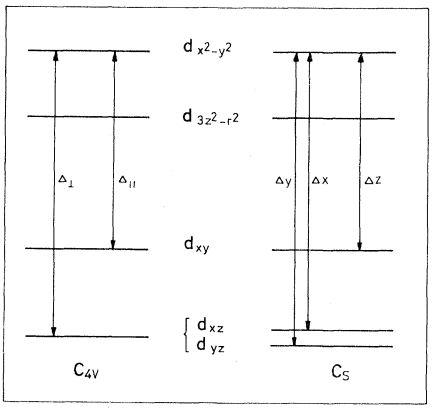

FIG. 10. Energy-level diagram for d electrons in a C_{4v} and in a C_s symmetry.

$\Delta_\perp$ an average of Δ_x and Δ_y, and for $\Delta_\parallel$ the Δ_z value. With these approximations we get

$$g_x = 2 - \frac{2\lambda}{\Delta_x} - 4\left[\frac{\lambda}{\Delta_z}\right]^2,$$
$$g_y = 2 - \frac{2\lambda}{\Delta_y} - 4\left[\frac{\lambda}{\Delta_z}\right]^2, \quad (4)$$
$$g_z = 2 - \frac{8\lambda}{\Delta_z} - 3\left[\frac{2\lambda}{\Delta_x + \Delta_y}\right]^2 - \frac{8\lambda^2}{\Delta_z(\Delta_x + \Delta_y)}.$$

Using these expressions with the values of g_x, g_y, and g_z given in Table I, we obtain $\Delta_x = 7700\ \text{cm}^{-1}$, $\Delta_y = 8100\ \text{cm}^{-1}$, and $\Delta_z = 5850\ \text{cm}^{-1}$.

As in the tetragonal case, the transitions associated with these energy differences are intraconfigurational and have not been observed due to their weakness. The uv absorption band at 285 nm will correspond to an interconfigurational transition, and from the dichroism experiments it is also concluded that it has a predominant σ character.

From the previous treatment the position of the d_{z^2} level cannot be checked, but it is clear that this level is not the highest one because in such a case the g values would be very different,[17] so the unpaired electron is in a $d_{x^2-y^2}$ orbital, which has a strong overlapping with the fluorine ligands, and this can be the reason for the observed structure of the defect in which only the hyperfine interaction with four fluorines is observed. It is also clear from this model that the electronic spin of the defect is $S = \frac{1}{2}$, which corresponds to that used in the spin Hamiltonian, which explains the experimental results.

ACKNOWLEDGMENTS

We are indebted to Mr. P. Wesseling for growing the crystals. We also thank Junta de Energia Nuclear (JEN) and Consejo Superior de Investigaciones Cientificas (CSIC) (Spain) for financial support.

[1]W. Gehlhoff and W. Ulrici, Phys. Status Solidi B 102, (1980).
[2]D. S. McClure and Z. Kiss, J. Chem. Phys. 39, 3251 (1963).
[3]J. L. Merz and P. S. Persahn, Phys. Rev. 162, 217 (1967).
[4]J. L. Merz and P. S. Persahn, Phys. Rev. 162, 235 (1967).
[5]D. L. Steabler and S. E. Schnatterly, Phys. Rev. B 3, 516 (1971).
[6]C. H. Henderson and E. S. Sabisky, Phys. Rev. B 3, 527 (1971).
[7]R. Alcalá and P. J. Alonso, J. Lumin. 20, 1 (1979).
[8]R. Alcalá, P. J. Alonso, G. Lalinde, and A. Carretero, Phys. Status Solidi B 98, 315 (1980).
[9]R. Alcalá and P. J. Alonso, J. Phys. C 13, 6049 (1980).
[10]J. M. Orera, R. Alcalá, and P. J. Alonso, J. Phys. D 14, 1923 (1981).
[11]P. J. Alonso, J. Casas-González, H. W. den Hartog, and R. Alcalá, Phys. Status Solidi B 100, 721 (1980).
[12]J. Casas-González, H. W. den Hartog, and R. Alcalá, Phys. Rev. B 21, 3826 (1980).
[13]F. Keffer, T. Oguchi, W. O'Sullivan, and Y. Yamashita, Phys. Rev. 115, 1553 (1959).
[14]A. Abragam and B. Bleamey, *Electron Paramagnetic Resonance of Transition Ions* (Clarendon, Oxford, 1971), Chap. 3.
[15]M. Moreno, An. Fis. 70, 261 (1974).
[16]H. Bill, Phys. Lett. 44A, 101 (1973).
[17]W. Hayes and J. Wilkens, Proc. R. Soc. London Ser. A 281, 340 (1964).